Int. J. Heat Mass Transfer. Vol. 28, No. 6, pp. 1057–1066, 1985
Printed in Great Britain

0017 9310/85 $3.00 + 0.00

Use of an adaptive grid procedure for parabolic flow problems

S. ACHARYA* and S. V. PATANKAR
Department of Mechanical Engineering, University of Minnesota, Minneapolis, MN 55955, U.S.A.

(*Received* 12 *May* 1983 *and in final form* 25 *October* 1984)

Abstract—An adaptive grid procedure is devised for the calculation of two-dimensional parabolic flows. The procedure redistributes the nodal points at each streamwise location of the flow so as to provide a finer mesh spacing in regions of rapid profile variation. Guidance is taken from the behavior of each dependent variable in deciding the final distribution of nodal points. Thus, critical regions in the flow field are always accurately resolved. It is shown that conventional differencing schemes do not perform satisfactorily on skewed grids, which are inherently associated with the adaptation procedure. A more suitable differencing scheme, which gives stable and accurate results, is developed. By means of various test problems, the improvement in results obtained by the adaptive grid procedure is demonstrated.

INTRODUCTION

IN MANY flow and heat transfer problems, physically important regions occur where the dependent variables exhibit large changes in gradient and/or curvature. In the numerical solution of such problems, satisfactory numerical accuracy can be obtained only if one provides a fine mesh spacing in these regions. But quite often, the location of a high-gradient or a high-curvature region is not known *a priori*. Therefore, a predetermined distribution of nodal points is either inadequate or computationally wasteful. What is needed is a method wherein the distribution of nodal points is continuously adjusted in response to the nature of the computed solution. By this procedure, it is possible to generate a mesh, which at all times concentrates the nodal points in the crucial regions. Such a method is called an adaptive grid procedure.

There are many practical situations where an adaptive grid procedure is especially beneficial. In combustion problems, the flame front is characterized by large gradients and curvature and continuously advances with time. In melting or freezing problems, the moving phase-change boundary plays a similar role. In heat exchanger applications, the boundaries are intentionally made discontinuous in order to augment heat transfer. At each discontinuity, new boundary layers (which are regions of steep gradients) are created.

The need for adaptation in many problems of interest has resulted in a systematic effort to develop suitable adaptation procedures. Bonnerot and Jamet [1, 2] have used space–time finite elements for the solution of the Stefan problem. Mori [3], Lynch and Gray [4, 5] and Lynch and O'Neill [6] have used continuously deforming finite elements in space and finite difference techniques for the integration in time. Miller and Miller [7] have also developed a moving finite element method which was later modified by Miller [8] and used by Gelinas *et al.* [9] and Djomehri [10]. Babuska and Rheinboldt [11, 12] have developed a theory of *a posteriori* error estimates to help design an optimal grid. Pereyra and Sewell [13], White [14] and Pierson and Kutler [15] have each used the idea of equidistributing an estimate for the truncation error. Olsen [16], Chong [17], Dwyer *et al.* [18], and Rai and Anderson [19] have developed adaptation procedures by providing a finer mesh in regions of large spatial gradients.

Most of the published literature deals with adaptation based on a single dependent variable. In addition, many of the investigations (e.g. [17, 18]) report problems arising from numerical instability. The motivation for the present work is to develop a simple, economical and stable adaptation procedure that will account for the profile variations of each dependent variable. Only two-dimensional parabolic flows with adaptation along the cross-stream coordinate are considered.

The basic calculation procedure used here for a parabolic flow problem is due to Patankar and Spalding [20]. This is an implicit finite difference marching procedure with the streamwise coordinate X and the cross-stream coordinate $\omega(=\psi-\psi_I/\psi_E-\psi_I)$ as the independent variables. At each downstream step, the governing partial differential equations are integrated over control volumes laid out as shown in Fig. 1. This yields a system of tri-diagonal algebraic equations which are solved by using the Thomas algorithm.

The salient features of adaptation procedure developed in the present work is described next. Further details of the method can be found in [21].

ADAPTATION PROCEDURE

To explain the adaptation procedure, it is convenient to introduce the concept of a computational coordinate η, although it does not directly participate in the discretization process. The computational coordinate η

* Present address: Department of Mechanical Engineering, Louisiana State University, Baton Rouge, LA 70803, U.S.A.

NOMENCLATURE

A_1	pre-exponential constant, equations (11) and (12)
f	ratio of the number of nodes in a coarse grid to the number of nodes in the corresponding adaptive grid
$F(Y)$	adaptation criterion
k	thermal conductivity
L/H	aspect ratio in an interrupted wall channel
Nu	Nusselt number
P	dimensionless pressure
Pr	Prandtl number
Q	strength of a point heat source, equation (4)
Re	Reynolds number
t	time
T	temperature
T_0	initial temperature, equation (4)
T_w	wall temperature, equation (8)
T_δ	free-stream temperature, equation (9)
U, V	X- and Y-direction velocities
U_δ	free-stream velocity, equation (9)
X, Y	coordinate directions
Y_j, Yf_j	value of Y at a node point j and the value of Y at the control-volume face below j
Y_{max}	maximum value of Y.

Greek symbols

α	thermal diffusivity
$\Delta\eta_{ij}$	computed increment in η at a node j and associated with a variable ϕ_i
$\Delta\tilde{\eta}_j$	computed increment in η at a node j and associated with the variable that advocates the densest clustering at j
$\Delta\eta_j^u$	computed uniform increment in η (with $F(Y) = 1$)
$\underline{\Delta\eta_j}$	rescaled values of $\Delta\tilde{\eta}_j$, equation (3)
ε	percentage error in local Nusselt number
η	computational coordinate, equation (1)
$\underline{\eta f_j}$	values of η at control volume faces and computed from $\underline{\Delta\eta_j}$ values
μ	viscosity
θ_1	constant, equations (11) and (12)
ρ	density
ρ_A	species concentration of A
ϕ	general dependent variable
ϕ_i	particular dependent variable
ω	dimensionless cross-stream coordinate, $\psi-\psi_I/\psi_E-\psi_I$
ωf_j	ω-value at control volume face below node j
ψ	stream function value
ψ_I, ψ_E	value of ψ at the internal and external boundaries.

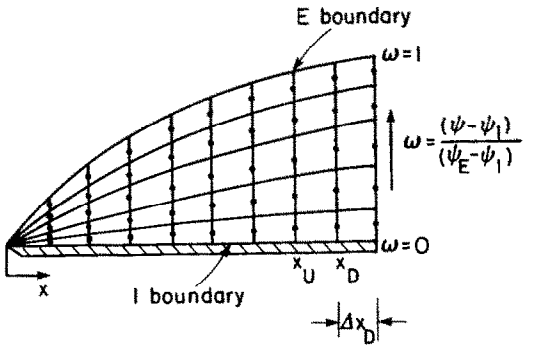

FIG. 1. The X–ω grid for the boundary layer on a flat plate.

is related to the physical coordinate Y according to the following equation

$$\eta = \int_0^Y F(Y)\,dY \Big/ \int_0^{Y_{max}} F(Y)\,dY. \qquad (1)$$

The function $F(Y)$ is called the adaptation criterion and is expected to be positive everywhere. The choice of $F(Y)$ describes how the nodal points in the physical space are distributed. The denominator in equation (1) is introduced to normalize the computational coordinate so that η always goes from 0 to 1.

Without any loss of generality, the nodal points can conveniently be assumed to be uniformly distributed in the η space. If $F(Y)$ is equal to a constant [Fig. 2(a)], then equation (1) prescribes a uniform nodal distribution in the physical space. If $F(Y)$ is not a constant [Fig. 2(b)] then the physical location of the nodal points is nonuniform. Further, the regions with large $F(Y)$ are associated with a fine distribution in the physical space. Thus, the key to obtaining an optimal mesh lies in an appropriate choice of $F(Y)$.

A mesh is considered to be optimal if it accurately resolves local regions of large gradients and curvatures. The logical choices for $F(Y)$ are, therefore, the gradient $\partial\phi/\partial Y$, and the curvature $\partial^2\phi/\partial Y^2$, where ϕ is the

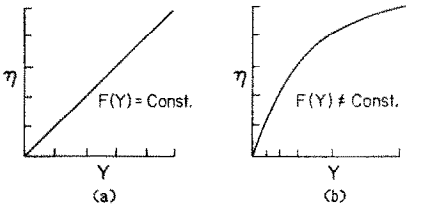

FIG. 2. The $\eta \sim Y$ relationship: (a) $F(Y) = 1$; (b) $F(Y) \neq 1$.

relevant dependant variable. In the basic finite difference method, a linear profile is assumed to exist between any two adjacent nodal points. If $\partial\phi/\partial Y$ does not vary significantly between the two points, the linear-profile assumption is reasonable. If, however, there is a rapid change in $\partial\phi/\partial Y$, a finer grid is necessary in this region so that a linear profile continues to be satisfactory. Therefore, $|\partial^2\phi/\partial Y^2|$, which is a measure of the rate of change of $\partial\phi/\partial Y$, is chosen here as the adaptation criterion $F(Y)$.

Although the curvature $|\partial^2\phi/\partial Y^2|$ is used as the primary adaptation criterion for the results presented in this paper, it should be pointed out that in many problems the regions of large $|\partial^2\phi/\partial Y^2|$ coincide with the regions of large $|\partial\phi/\partial Y|$. In such situations, the use of $|\partial\phi/\partial Y|$ as the adaptation criterion is not inappropriate.

In equation (1) it is required to determine the Y values for uniformly specified η. However, the procedure to be followed here is to first calculate η from the available $\phi \sim Y$ distribution (either the upstream solution or a downstream solution based on an *a priori* grid) thereby establishing the $\eta \sim Y$ (or ω) relationship. Then, for uniformly specified η values, the corresponding Y (or ω) values are obtained by suitable interpolation.

The adaptation criterion is to be calculated for each dependent variable ϕ_i and at each cross-stream location Y_j. This can be done by any reasonable method. The procedure adopted here is to use the monotonic cubic interpolation scheme of Fritsch and Carlson [22] to fit the $\phi_i \sim Y_j$ data. This yields the $(\partial\phi_i/\partial Y)_j$ values. Central differences of the first derivatives are then used to obtain $(\partial^2\phi_i/\partial Y^2)_j$, the absolute value of which represents the magnitude of the primary adaptation criterion.

A flow and heat transfer problem typically requires the solution of momentum and energy equations. In certain situations, differential equations for other variables, such as chemical species concentration, turbulence quantities, etc. have to be solved. For each dependent variable, equation (1) defines a unique $\eta \sim Y$ relationship. The final $\eta \sim Y$ relation should ideally satisfy the individual demands for grid refinement made by each dependent variable. To accomplish this, each physical location is considered in turn and the dependent variable which advocates the smallest mesh size (in the physical space) at that location is used in the definition of the adaptation criterion.

To implement the above idea, it is convenient to write equation (1) for each control volume and to express the integral in the numerator as the sum of two integrals. This gives

$$\Delta\eta_{ij} = \left\{ \int_{Yf_j}^{Y_j} |(\partial^2\phi_i/\partial Y^2)_j| \, dY + \int_{Y_j}^{Yf_{j+1}} |(\partial^2\phi_i/\partial Y^2)_j| \, dY \right\} \div \int_0^{Y_{max}} |(\partial^2\phi_i/\partial Y^2)_j| \, dY \quad (2)$$

where $\Delta\eta_{ij}$ is the computational mesh size calculated for the dependent variable ϕ_i at the cross-stream location Y_j. Each integral is evaluated by first expressing the $|(\partial^2\phi_i/\partial Y^2)_j| \sim Y_j$ variation by the cubic interpolating curve in [22]. This permits the integrals in equation (2) to be expressed in terms of known quantities. Each column of the two-dimensional array $\Delta\eta_{ij}$ corresponds to a particular cross-stream location (characterized by subscript j) while each entry in the column is the mesh size (at that location) advocated by a dependent variable (ϕ_i). If the largest entry in each column is chosen and normalized, a one-dimensional array (say $\Delta\tilde{\eta}_j$) is obtained, each element of which corresponds to a particular cross-stream location (j) and contains the value of the mesh size advocated by the dependent variable which has the largest profile curvature at that point.

In certain situations, the sole use of $|\partial^2\phi/\partial Y^2|$ as the adaptation criterion was found to produce excessively skewed grids. Although an appropriate amount of stretching is desirable, excessive stretching could produce mesh sizes in the round-off error range and could also result in errors due to inaccurate interpolation. To avoid such problems, an additional constraint on the grid distribution needs to be imposed. This is done by using another adaptation criterion $F(Y) = 1$ in conjunction with $F(Y) = |\partial^2\phi/\partial Y^2|$. With $F(Y) = 1$, the computational mesh sizes as computed from equation (1) are all of the same size (say $\Delta\eta_j^u$). A mesh size $\Delta\eta_j$ is then computed as

$$\Delta\eta_j = \text{Greater of } (\Delta\tilde{\eta}_j, \Delta\eta_j^u) \div \sum_j \text{Greater of } (\Delta\tilde{\eta}_j, \Delta\eta_j^u). \quad (3)$$

The resulting grid has less drastic nonuniformity than does the grid defined by equation (2). With the computational mesh sizes as calculated from equation (3) the coordinate values ηf_j at the control volume face location can be obtained as

$$\eta f_j = \eta f_{j-1} + \Delta\eta_j \quad (3')$$

with the starting value of ηf set equal to zero at the $\omega = 0$ boundary. This procedure provides the necessary constraint needed to design an appropriately skewed grid.

The computational coordinate ηf_j corresponds to a physical location Yf_j (or ωf_j). In the basic finite difference calculation procedure [20] the ω-values at the downstream step are needed and so the adapted mesh must be described in terms of ω-values.

A relationship between the computational and physical space is established by using the Fritsch–Carlson monotonic interpolating curve [22] to define a polynomial relationship between the ηf_j, obtained from equation (3'), and the corresponding ωf_j values. It is important to use a monotonic interpolating curve since for increasing values of the computational coordinate the physical coordinate can only increase. As mentioned earlier, the adaptation procedure is based

on calculating the physical locations that correspond to a uniformly specified computational mesh. Hence, the cubic interpolating curve (between ηf_j and ωf_j) obtained as described above, is used to calculate the new ωf values that correspond to uniformly increasing values of the computational coordinate. These ωf values describe the adapted mesh at the downstream location.

In every marching step of the parabolic flow calculation, the $\phi_i \sim Y_j$ distribution at an upstream station is known and the distribution at the next downstream station is to be calculated. In the present procedure it was initially decided that the $(\partial^2\phi_i/\partial Y^2)_j$ values would be evaluated from the upstream $\phi_i \sim Y_j$ distribution. This would permit a dynamic adaptation, i.e. no *a priori* evaluation of the solution at the downstream step is needed to determine the grid distribution. However, this procedure led to oscillations between the adapted grid and the solution. Dwyer *et al.* [18] have encountered similar problems. The remedy they adopt is to perform the adaptation less frequently, i.e. once every four forward steps.

It is, of course, desirable to have a procedure that adapts at every forward step so that the large curvature regions are always appropriately accounted for. Also, the adaptation scheme should be stable since oscillatory solutions are obviously unacceptable.

The adaptation procedure developed here involves obtaining two solutions in parallel. First, a *coarse* predetermined grid solution is obtained; it provides the inputs from which the $(\partial^2\phi_i/\partial Y^2)_j$ values and thus the adapted grid can be determined. Then, the main solution is obtained on the adapted grid. This procedure is repeated at every forward step, with the predetermined grid solution immediately preceding the adaptive grid solution. In essence, this procedure decouples the calculation of the adapted grid from the solution of the differential equations on the adapted grid. Thus, the oscillations associated with the adaptive grid based on the upstream solution are eliminated.

It should be mentioned that this procedure involves additional computational work for obtaining the solution on the predetermined grid. But, a relatively coarse predetermined grid is found to suffice, since the corresponding solution is used only for defining an interpolating curve from which the values of $(\partial^2\phi_i/\partial Y^2)_j$ are evaluated. Hence, if the adaptive grid has N nodal points, the predetermined grid need only have fN nodes, where $f < 1$. The number of equations to be solved is then $(1+f)N$ which is less than the $2N$ equations required to be solved in many other adaptation procedures [7–10, 15, 16]. Usually, a satisfactory value of f is 0.4 or less.

CHOICE OF A DIFFERENCING SCHEME

In the discretization of the governing differential equations, a control volume approach is used, where profile assumptions are used in both the streamwise and the cross-stream directions. The accuracy of the calculation procedure depends on the choice of profile assumptions.

In the conventional definition of a control volume, the control volume face between the downstream nodes j and $j+1$ also lies between the same upstream nodes. An example is the Patanker–Spalding method [20] where lines of constant ω are used to define the cross-stream control volume faces (see Fig. 1). In a similar fashion, the present work was initiated with control volumes bounded by lines of constant η [Fig. 4(a)]. Since, in general, the distribution of nodal points in the physical space can drastically change from one station to the next, the lines of constant η are likely to be more oblique in the physical space than the lines of constant ω or Y. As a result, there could be significant mass flow crossing the constant-η lines. Thus, how the cross-stream convection (with the associated diffusion) is handled by the differencing scheme becomes more important for the X–η grid than for the X–ω or the X–Y grid.

To determine the most appropriate differencing scheme, a model test problem with a known analytical solution was solved using a number of differencing schemes. The choice of the differencing scheme is based on the accuracy of the results obtained.

The test problem is that of a uniform, unidirectional flow past a point heat source of strength Q. The exact solution for the temperature T can be written as

$$T - T_0 = \frac{Q}{2\sqrt{\pi k X}} e^{-Y^2/4kX} \tag{4}$$

where T_0 is the initial (upstream) temperature of the fluid and k is the thermal conductivity. The calculation is initiated at $X = X_0$ with the starting condition obtained from equation (4). Values of the heat source strength Q, and the location $X = X_0$ may be specified arbitrarily.

The streamwise convection at the upstream and downstream faces of the control volume was calculated by assuming a stepwise profile, in which the convected value of ϕ was taken to be the nodal value of ϕ located on the control-volume face. For the convection and diffusion across the cross-stream faces of the control volume, the following profile assumptions were tried:

1. Explicit convection/Crank–Nicholson diffusion.
2. Explicit convection/implicit diffusion.
3. Crank–Nicholson convection/implicit diffusion.
4. Crank–Nicholson convection/Crank–Nicholson diffusion.
5. Implicit exponential scheme.

The explicit terms are calculated from the known upstream solution while the implicit convection and diffusion fluxes are expressed in terms of the unknown downstream values. The Crank–Nicholson convection and diffusion terms are obtained as a mean of the upstream and downstream values. In the implicit exponential scheme, the total flux (convective plus diffusive flux) across the cross-stream face is obtained from the exact solution of the one-dimensional

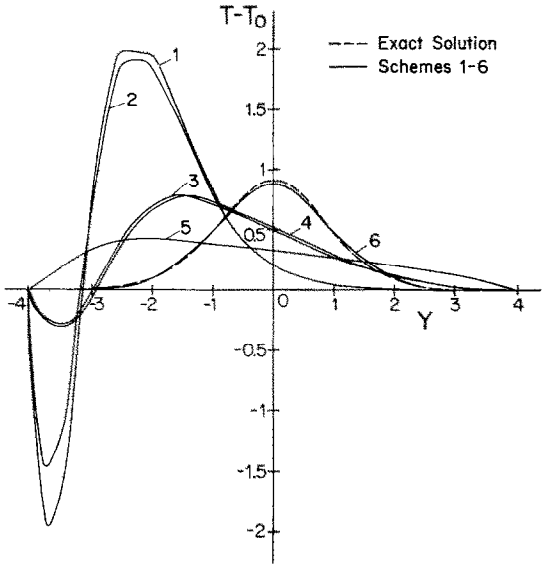

FIG. 3. Performance of various differencing schemes.

convection–diffusion equation (at the downstream location). This scheme was first proposed by Spalding [23] and has been widely used.

The calculation is done on a grid that is appreciably skewed. The exact solution at a certain X [equation (4)] and the corresponding results obtained by using schemes 1–5 are plotted in Fig. 3. It can be seen that none of the schemes 1–5 appear to produce reasonable solutions. Schemes 1–4 give negative values which are obviously unrealistic. Scheme 5 appears to produce a 'smeared' profile, indicative of appreciable false diffusion.

Evidently, there is a need for a more satisfactory scheme. Experience with schemes 1–4 indicates that as the inclination of the control volume faces (in the physical plane) is reduced, all schemes give more satisfactory results. This is particularly true for scheme 5, which for small inclination of control volume faces gives results very close to the exact solution.

Guidance is taken from these experiences to construct a new scheme called the ω-tracing scheme. The central idea in the new scheme is to modify the definition of the control volume faces. Instead of lines of constant η, the control volume faces are taken to be constant ω lines originating from the interface locations between the downstream nodal points and traced backwards to the upstream station [Fig. 4(b)]. Since the ω-values of the downstream nodal points are different from the ω-values of the corresponding upstream nodes (due to cross-stream adaptation) a typical control volume in the ω-tracing scheme will contain a nodal point on the downstream face but may contain any number of nodal points (including zero) on the upstream face. This complicates the calculation of the upstream streamwise convection, which now must be obtained by suitable interpolation. The piecewise cubic interpolating curve in [22] is once again employed for this purpose. The cross-stream convection and diffusion terms are calculated implicitly by the exponential scheme.

The results of this method (called scheme 6) are also shown in Fig. 3. The solution obtained is very accurate and obviously superior to the other methods discussed (schemes 1–5). Therefore, scheme 6 is adopted for implementation in the calculation procedure.

RESULTS

To demonstrate the improvements obtained by the grid adaptation procedure, a variety of problems have

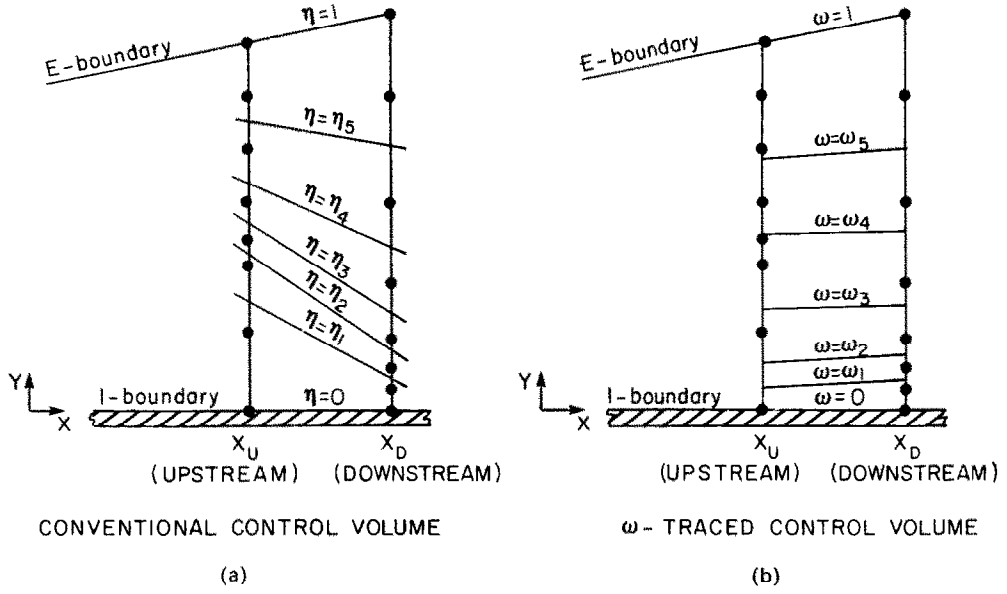

FIG. 4. Conventional and ω-traced control volumes.

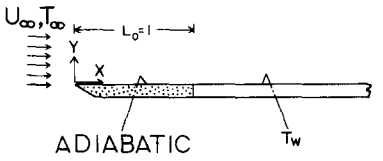

FIG. 5. Test problem 1. Flate plate with an unheated starting length.

been solved both on an adaptive grid and on a fixed grid. The results obtained have been compared with an exact solution. In all the test problems, the forward step sizes chosen are of the order of 10^{-5}. Further reduction in the forward step size had a negligible influence on the results. The test problems chosen are representative of the multitude of flow and heat transfer problems encountered in many practical situations.

Test problems

1. *Flat plate with an unheated starting length.* Figure 5 shows the physical situation which schematically represents the flow over a flat plate with an unheated starting length. When the flow encounters the point of thermal discontinuity, a thin thermal boundary layer develops. To accurately resolve this region, a fine mesh spacing is necessary near the heated wall. As the thermal layer grows, the grid needs to expand so as to correctly account for the entire thermal layer. The adaptive grid procedure is expected to provide the correct cross-stream distribution of nodal points at each streamwise location.

To obtain the desired solution, the equations expressing the conservation of mass, momentum and energy have to be solved. These are

$$\frac{\partial U}{\partial X} + \frac{\partial V}{\partial Y} = 0, \tag{5}$$

$$U\frac{\partial U}{\partial X} + V\frac{\partial U}{\partial Y} = \frac{\mu}{\rho}\frac{\partial^2 U}{\partial Y^2}, \tag{6}$$

$$U\frac{\partial T}{\partial X} + V\frac{\partial T}{\partial Y} = \alpha\frac{\partial^2 T}{\partial Y^2}. \tag{7}$$

The boundary conditions are,

at $Y = 0$,

$$U = 0$$

$$\frac{\partial T}{\partial Y} = 0 \quad \text{for} \quad 0 \leqslant X < 1 \tag{8}$$

$$T = T_w \quad \text{for} \quad X \geqslant 1$$

at $Y = Y_\delta$,

$$U = U_\delta, \quad T = T_\delta \quad \text{for all } X. \tag{9}$$

The adaptive grid and the fixed grid solutions are both obtained with 20 grid points. The results predicted by Abdel-Wahad *et al.* [24] are re-evaluated by using 300 grid points in a fixed grid method. These results are used as the exact solution for the purpose of determining errors.

Figure 6 shows the distribution of the nodal points at various streamwise locations. At $X = 1$, the onset of the constant temperature boundary condition and the ensuing rapid profile variations cause a dense clustering of nodal points near the wall. As the thermal boundary layer grows the nodal points appropriately spread out.

For the purpose of comparing the relative accuracy of the computed solutions, the percentage error in the local Nusselt number along the thermally active plate is

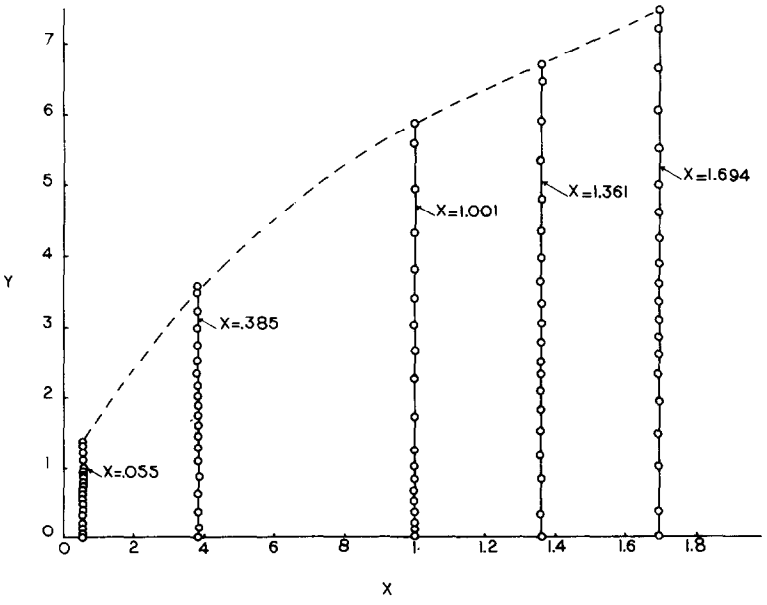

FIG. 6. Nodal point distribution in test problem 1.

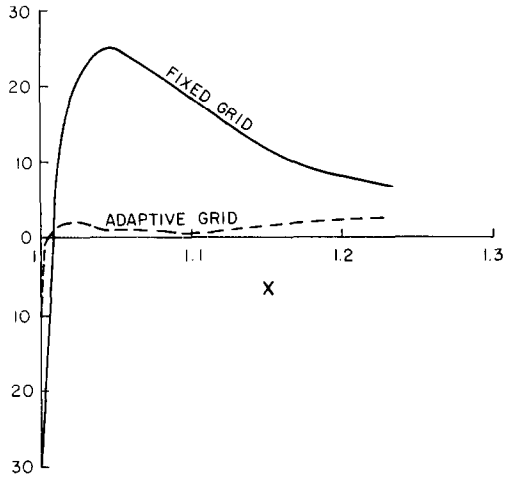

FIG. 7. Percentage error of the local Nusselt number along the thermally active plate in test problem 1.

plotted in Fig. 7. While the errors incurred in the fixed grid method (solid line) are as large as 25%, the adaptive grid solution (dashed line) has a maximum error of about 3%. The fixed grid method is found to be especially inadequate over the initial thermally developing region.

2. *Interrupted wall channel.* In an interrupted wall channel, the solid boundaries of a parallel plate channel are interrupted periodically in the streamwise direction. Such a configuration is commonly used to augment heat transfer since the periodic interruptions are associated with creation of new boundary layers and therefore higher heat transfer coefficients.

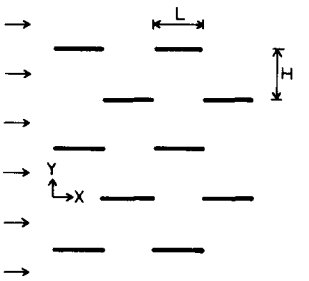

FIG. 8. Test problem 2. An interrupted wall channel.

A schematic of the physical situation is shown in Fig. 8. Over each plate, the near wall regions close to the leading edge are associated with rapid profile variations and therefore demand a fine mesh spacing. Locations far removed from the wall have mild profile variations and therefore a coarse mesh should suffice in those regions.

The solutions are again obtained by numerically integrating equations (5)–(7). The boundary conditions are zero velocity and temperature at the walls and zero gradients at the symmetry line.

Both the fixed grid and the adaptive grid solution are obtained using 32 cross-stream nodal points. Figure 9 plots the nodal point locations (Y/H) of the adaptive grid at different streamwise positions (X/H). As may be seen, the grid is automatically rezoned at each forward step, in order to provide a fine mesh in regions of large curvature.

For the purpose of comparing results, an exact Nusselt number is calculated by using 300 cross-stream nodal points in a fixed grid method. The Nusselt

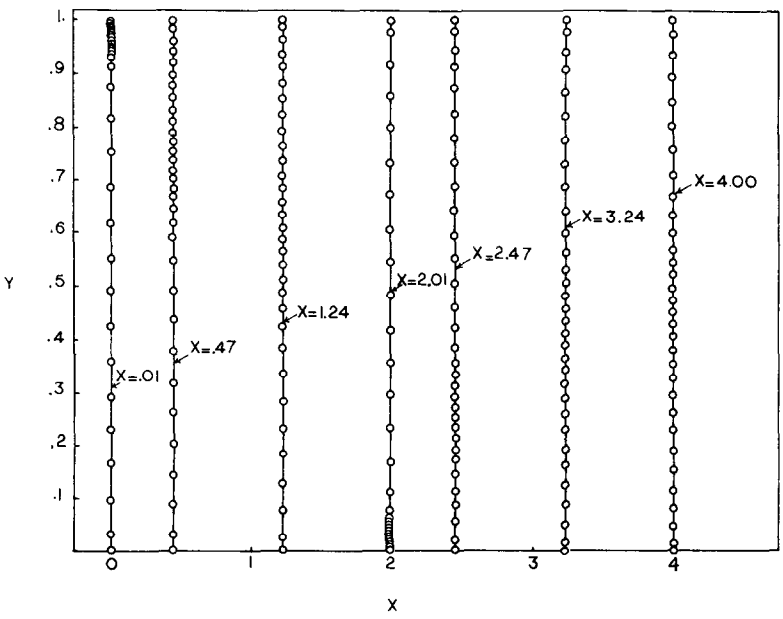

FIG. 9. Nodal point distribution in test problem 2.

Table 1. Percentage error in the fully developed Nusselt number in test problem 2

	% Error in Nusselt number	
Re Pr/(L/H)	Fixed grid	Adaptive grid
28	1.60	0.00
70	2.50	0.00
140	3.30	0.00
280	4.23	0.05
560	5.11	0.21
1400	5.02	0.36
2800	3.45	0.87

number (at a downstream step) is defined as in [25] and takes the following form,

$$Nu = [Re\ Pr/(L/H)] \ln [(T_w - T_b)'/(T_w - T_b)''] \quad (10)$$

where $(T_w - T_b)''$ is the wall to bulk temperature difference at the downstream step and $(T_w - T_b)'$ is the temperature difference at the corresponding step of the previous plate. When flow is fully developed, the Nusselt number becomes a constant.

The percentage error in the fully developed Nusselt number is tabulated against $Re\ Pr/(L/H)$ in Table 1. These results again demonstrate the improvements obtained by using the adaptive grid method.

3. *One-dimensional combustion in a solid material.* This problem was earlier investigated by Otey and Dwyer [26] to test the efficiency of five numerical procedures. They have considered a slab of material A heated from the right hand side. As the temperature rises material A decomposes to material B. A reaction zone, characterized by large curvatures, proceeds through the slab until all of material A is converted to B.

This problem may be modelled as a transient

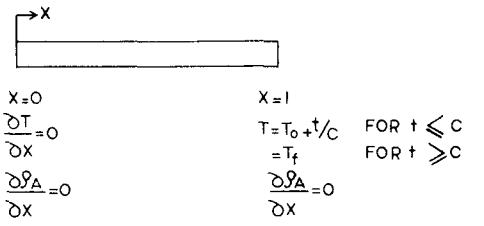

FIG. 10. Test problem 3. One-dimensional combustion in a solid material.

diffusion equation with Arrhenius type source terms. If T and ρ_A denote the temperature and species concentration of A, then the problem is described by the following equations:

$$\frac{\partial \rho_A}{\partial t} = \frac{\partial^2 \rho_A}{\partial X^2} - A_1 \rho_A e^{-\theta_1/T}, \quad (11)$$

$$\frac{\partial T}{\partial t} = \frac{\partial^2 T}{\partial X^2} + A_1 \rho_A e^{-\theta_1/T}. \quad (12)$$

The boundary conditions to be used are indicated in Fig. 10. While the left hand boundary is held adiabatic, the right hand boundary is heated so that the temperature rises linearly up to a time $t < c$ beyond which it is held fixed at T_f. The values of the parameters in the problem are chosen from those used by Otey and Dwyer [26].

It is possible to use the two-dimensional boundary-layer procedure to solve the one-dimensional unsteady problem by replacing $U\ \partial/\partial X$ in the boundary layer case by $\partial/\partial t$ for the unsteady situation.

In Fig. 11, the temperature distribution at two

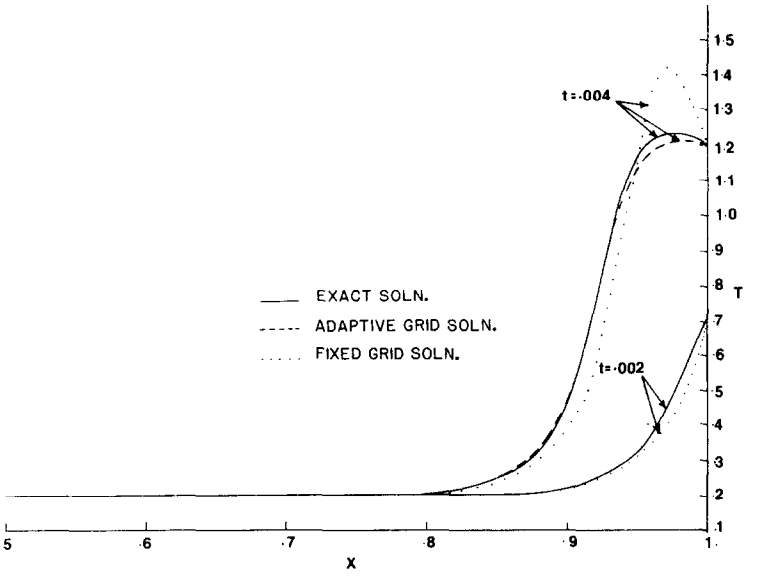

FIG. 11. Temperature distribution in test problem 3.

instances of time are compared with the exact solution. Both the fixed grid and the adaptive grid solutions are based on 20 nodal points while the exact solution is obtained by using 300 cross-stream nodal points in a fixed-grid calculation. Again the adaptive grid results (dashed lines) lie much closer to the exact solution (solid lines) than the fixed grid results (dotted lines).

CLOSING REMARKS

An adaptive grid procedure is developed and implemented for parabolic flows. The procedure, which takes guidance from each dependent variable, clusters the nodal points in regions of large curvatures. The conventional differencing schemes are found to yield inaccurate solutions on an adapted grid. A new differencing scheme called the ω-tracing scheme is developed and shown to produce accurate solutions. Results of three test problems are presented to demonstrate the improvements in accuracy obtained with the adaptive grid procedure.

REFERENCES

1. R. Bonnerot and P. Jamet, A second order finite element method for the one-dimensional Stefan problem, *Int. J. num. Meth. Engng* **8,** 811–820 (1974).
2. R. Bonnerot and P. Jamet, A third order discontinuous finite element method for the one-dimensional Stefan problem, *J. Comp. Phys.* **32,** 145–167 (1979).
3. M. Mori, A finite element method for solving moving boundary problems, *Int. Federation for Information Processing Congress on Modelling of Environmental Systems*, Tokyo, pp. 167–171 (1967).
4. D. R. Lynch and W. G. Gray, Finite element simulation of flow in deforming regions, *J. Comp. Phys.* **36,** 135–153 (1980).
5. D. R. Lynch and W. G. Gray, Finite element simulation of shallow water problems with moving boundaries, in *Finite Elements in Water Reservoirs*, Vol. II (edited by C. A. Brebbia, W. G. Gray and G. F. Pinder), Pentech Press, London (1978).
6. D. R. Lynch and K. O'Neill, Continuously deforming finite elements for the solution of parabolic problems, with and without phase change, *Int. J. num. Meth. Engng* **17,** 81–96 (1981).
7. L. Miller and R. N. Miller, Moving finite elements. I, *SIAM J. num. Anal.* **18,** 1019–1032 (1981).
8. K. Miller, Moving finite elements. II, *SIAM J. num. Anal.* **18,** 1033–1057 (1981).
9. R. J. Gelinas, S. K. Doss and K. Miller, The moving finite element method : application of general partial differential equations with multiple gradients, *J. Comp. Phys.* **40,** 202–249 (1981).
10. M. J. Djomehri, Moving finite element solution of systems of partial differential equations in 1-dimension, Ph.D. thesis, University of California, Berkely (1981).
11. I. Babuska and W. C. Rheinboldt *A posteriori* error estimates for the finite element method, *Int. J. num. Meth. Engng* **12,** 1597–1615 (1978).
12. I. Babuska and W. C. Rheinboldt, Error estimates for adaptive finite element computations, *SIAM J. num. Anal.* **15,** 736–754 (1978).
13. V. Pereyra and E. G. Sewell, Mesh selection for discrete solution of boundary value problems in ordinary differential equations, *Num. Math.* **23,** 261–268 (1975).
14. A. B. White, On selection of equidistributing meshes for two point boundary value problems, Center for Numerical Analysis, Report 112, University of Texas, Austin (1976).
15. B. L. Pierson and P. Kutler, Optimal nodal point distribution for improved accuracy in computational fluid dynamics, *A.I.A.A. Jl* **18,** 49–54 (1980).
16. J. J. Olsen, Subsonic and transonic flow over sharp and round nosed non-lifting airfoils, Ph.D. thesis, Ohio State University (1976).
17. T. H. Chong, A variable mesh finite difference method for solving a class of parabolic differential equations in one space variable, *SIAM J. num. Anal.* **15,** 835–857 (1978).
18. H. A. Dwyer, R. J. Kee and B. R. Sanders, Adaptive grid method for problems in fluid mechanics and heat transfer, *A.I.A.A. Jl* **18,** 1205–1212 (1980).
19. M. M. Rai and D. A. Anderson, Grid evolution in time asymptotic problems, *J. Comp. Phys.* **43,** 327–344 (1981).
20. S. V. Patankar and D. B. Spalding, *Heat and Mass Transfer in Boundary Layers* (1st edn). Intertext Publishers, London (1970).
21. S. Acharya, A calculation procedure for parabolic flows with adaptive grid and spline techniques, Ph.D. thesis, University of Minnesota, Minneapolis (1982).
22. F. N. Fritsch and R. E. Carlson, Monotone piecewise cubic interpolation, *SIAM J. Num. Anal.* **17,** 238–246 (1980).
23. D. B. Spalding, A novel finite difference formulation for differential expressions involving both first and second derivatives, *Int. J. num. Meth. Engng* **6,** 551–559 (1972).
24. R. M. Abdel-Wahad, E. M. Sparrow and S. V. Patankar, Mixed convection on a vertical plate with an unheated starting length, *J. Heat Transfer* **98,** 576–580 (1976).
25. E. M. Sparrow, B. R. Baliga and S. V. Patankar, Heat transfer and fluid flow analysis of interrupted wall channels, with application to heat exchangers, *J. Heat Transfer* **99,** 4–10 (1977).
26. G. R. Otey and H. A. Dwyer, Numerical study of the interaction of fast chemistry and diffusion, *A.I.A.A. Jl* **17,** 606–613 (1979).

UTILISATION D'UNE PROCEDURE A GRILLE ADAPTATIVE POUR DES PROBLEMES D'ECOULEMENT PARABOLIQUES

Résumé—Une procédure à grille adaptative est conçue pour calculer les écoulements bidimensionnels paraboliques. La procédure redistribue les points nodaux à chaque location de l'écoulement de façon à fournir une maille plus petite dans les régions de grande variation du profil. On tient compte du comportement de chaque variable pour décider de la distribution finale des points nodaux. Ainsi des régions critiques dans le champ de vitesse sont toujours traitées avec précision. On montre que les schémas conventionnels ne se comportent pas bien sur des grilles déformées qui sont associées de façon inhérente à la procédure d'adaptation. On développe un schéma plus convenable qui donne des résultats stables et précis. A partir de plusieurs problèmes, on démontre la qualité des résultats obtenus par la procédure à grille adaptative.

VERWENDUNG EINER ANPASSUNGSFÄHIGEN GITTERPROZEDUR BEI PARABOLISCHEN STRÖMUNGSPROBLEMEN

Zusammenfassung—Es wird eine anpassungsfähige Gitterprozedur zur Berechnung zweidimensionaler parabolischer Strömungen entworfen. Diese Prozedur verteilt die Knotenpunkte an jedem Ort der Strömung neu, so daß ein feinerer Gitterabstand in Gebieten mit starken Profiländerungen erzielt wird. Das Verhalten jeder abhängigen Variablen gibt eine Anleitung zur Wahl der endgültigen Verteilung der Knotenpunkte. Auf diese Weise werden kritische Gebiete im Strömungsfeld immer genau aufgelöst. Es zeigt sich, daß konventionelle Differenzenverfahren bei einem schiefen Gitter, das bei der Anpassungs-Prozedur zwangsläufig auftritt, nicht genügend wirksam sind. Es wird ein zweckmäßigeres Differenzenverfahren entwickelt, welches stabile und genaue Ergebnisse liefert. Die Verbesserung der Ergebnisse unter Verwendung der anpassungsfähigen Gitterprozedur wird mit verschiedenen Testproblemen nachgewiesen.

ПРИМЕНЕНИЕ АДАПТИРУЮЩИХСЯ СЕТОК ДЛЯ РАСЧЕТА ПАРАБОЛИЧЕСКИХ ТЕЧЕНИЙ

Аннотация—Разработана методика выбора адаптирующейся сетки для расчета двумерных параболических течений. Узловые точки перераспределяются в каждой направленной по течению области потока таким образом, чтобы обеспечить более частое расположение ячеек в зонах быстрого изменения профиля. Закономерность распределения узлов определяется поведением каждой зависимой переменной. Благодаря этому, критические области поля течения определяются точно. Показано, что общепринятые схемы дифференцирования неудовлетворительны для использования их на косых сетках, присущих данной методике. Разработана более подходящая схема дифференцирования, дающая устойчивые и точные результаты. При помощи различных тестовых задач продемонстрировано улучшение результатов, полученных на адаптирующихся сетках.